

OBJECTIVE IDENTIFICATION OF SUPERCELLULAR INTERNAL MOMENTUM SURGES USING A CLOUD MODEL

Matthew C. Mahalik* and Johannes M.L. Dahl

Atmospheric Science Group, Department of Geosciences, Texas Tech University, Lubbock, Texas

1. INTRODUCTION

Davies-Jones and Brooks (1993) established the well-known description of tornadogenesis as a three-step process. In Step 1, horizontal vorticity is tilted into the vertical by an updraft, forming a mid-level mesocyclone. Second, a downdraft produces vertical vorticity at the surface. The final step involves the tightening of vertical vortex lines through convergence and vertical stretching to the point where a surface vortex spins up. Among these steps, the most questions still lie within the second.

Work from Davies-Jones (1982), Davies-Jones and Brooks (1993), and others demonstrated the importance of downdrafts in tornadogenesis in the absence of preexisting low-level vorticity. More recent findings have identified rear-flank downdraft (RFD) surges as a key contributing factor (Markowski 2002), both in modeling (e.g., Schenkman et al. 2014) and observations (Lee et al. 2004, Marquis et al. 2008, Finley and Lee 2008, Skinner et al. 2014, among others). Far fewer studies have focused on the region north of the hook echo, where the primary precipitation core is located; the so-called forward-flank downdraft (FFD) originates from negative buoyancy in this region (Shabbott and Markowski 2006).

Dating back to Goff (1976), observations have shown fluctuations in outflow air within the cold pool, and additional modeling studies have presented evidence of surges within the forward flank, though these were often not the focus

of the work (Trapp and Weisman 2003, Dahl et al. 2014, and Schenkman et al. 2014).

Pulses of downdrafts result in bursts of strong outflow as particularly intense downdraft pulses reach the surface and spread out horizontally. These bursts manifest near the ground as wind speed and direction perturbations, and are referred to herein as internal momentum surges, or just surges. Previously identified internal momentum surges associated with downdraft pulsing are often accompanied by vertical vorticity extrema, of which some show a tendency to merge with and occasionally intensify preexisting near-ground vorticity (Dahl et al. 2014).

This study presents a method of objective identification of internal momentum surges generated in numeric simulations of a supercell. The algorithm aims to quantify surge characteristic frequency, magnitude, and source regions. A step-by-step description of the algorithm and an initial testing strategy are outlined in Section 2.

2. METHODS

This study employs the Bryan Cloud Model (CM1; Bryan and Fritsch 2002), version 16. Horizontal grid spacing is 250 m, and vertical grid spacing is stretched from 100 m in the lowest vertical slice to 250 m near the top of the domain. The base-state sounding replicates the 1977 Del City, OK, case (Brandes 1981). The storm is initialized from the introduction of a stationary, 4 km-diameter, 1400 m-deep bubble of air with a maximum 2 K temperature perturbation centered 1400 m AGL. Morrison double-moment microphysics is utilized. A still image showing the near-ground vertical vorticity distribution of the storm at peak intensity is shown in Figure 1.

*Corresponding author address: Matthew C. Mahalik, Texas Tech Univ., Dept. of Geosciences, Box 41053, Lubbock, TX 79409-1053; email: matthew.mahalik@ttu.edu.

In this study, horizontal momentum surges are defined as storm-relative velocity-magnitude perturbations in the lowest scalar vertical level (50 m AGL). In equation form,

$$S = (u'^2 + v'^2)^{\frac{1}{2}} \quad (1)$$

where u' and v' are the storm-relative perturbation velocities in x- and y-directions, respectively. The background flow is defined as the base-state mean wind, such that all perturbation to the flow is purely storm-generated. Average storm motion is subtracted such that the storm remains stationary and velocity perturbation is storm-relative.

An analysis subdomain is defined within the overall model domain. For these calculations, this inner domain is automatically centered on the primary downdraft in an attempt to identify the rate at which the most intense downdraft produces surges. The size of the subdomain is specified manually and varies by case, usually 5-10 km across: small enough to eliminate artifacts produced by processes unrelated to the downdraft being examined but sufficiently large to observe the evolution of surges following their genesis.

In the region immediately surrounding the source, outflow almost always generates flow radially outward throughout the majority of the domain. As a result, the subdomain configuration isolates surges generated by the designated source by minimizing the likelihood that surges from other, weaker downdraft sources enter the analysis region. Within the subdomain, a filter is applied to assign a binary "0" or "1" to all grid points, dependent on whether S is greater than a chosen threshold. In this study, a threshold of 13 m s^{-1} is implemented for a full-scale supercell simulation, similar to the threshold Lee et al. (2012) used to classify RFDs. This magnitude is large enough to filter out small-scale noise while still emphasizing the initial visually identifiable surges early in the storm's evolution. For demonstrative purposes, lower threshold magnitudes are implemented in test cases to

highlight the visual appearance of identified surges.

Following the identification of momentum surges, basic statistics of the features are generated, including total integrated horizontal extent of all surges in the subdomain, maximum and average surge intensity, and source location. An example of output statistics is shown in Figure 2. The surge source is assumed to be the location where downdraft intensity (i.e., negative vertical velocity) is greatest at $z = 1500 \text{ m}$. For the purposes of this study, only a single surge source is considered. While supercells in nature contain multiple downdrafts producing outflow, the scope of this study is to develop and test the technique's ability to identify the rate at which a typical, individual, thermodynamically-induced downdraft generates surges.

At each time step, a subdomain-integrated horizontal surge extent is calculated by summing the total number of grid points within the analysis region. This quantity is particularly relevant to the frequency of surge production by the pulsing downdraft. A horizontally integrated surge time series plot (Fig. 2a) visually represents new surge generation as peaks (an increased number of grid points affected by a surge), while dissipation or exit of a surge from the domain appears as a relative valley (fewer grid points affected). Fourier decomposition can then be applied to the resulting time series to identify dominant waveforms and frequency of surge "peaks."

Altering the size of the analysis subdomain influences the rate of surge flux out of the domain, affecting the shape of the total surge extent time series data. For example, larger domains allow surges to dissipate gradually, while smaller domains result in surges that exit through lateral boundaries before diminishing. As a result, smaller subdomains tend to produce a sharper, less-continuous time series. A storm with multiple downdrafts pulsing chaotically may result in a domain jumping between multiple source regions. This introduces the possibility that surges from different sources with potentially different

characteristics are sampled without differentiation. This and other limitations to the method outlined here are discussed further in Section 4.

The surge identification algorithm was subjected to a series of tests conducted using fully-idealized downdraft simulations, as described in Parker and Dahl (2014). These simulations used the same model parameters as the full-physics simulation described above, with the exception that isolated, dry downdrafts were forced artificially. Rather than initializing a warm bubble to produce a storm, a region of cooling is maintained aloft, governed by a sinusoidal variation, causing trajectories passing through to gain negative buoyancy and develop negative vertical velocity. The resulting dry downdrafts provide insight into outflow behavior, with highly detailed and complicated structure evident even with simple experiment design. Different downdraft characteristics were used to simulate varying outflow structure. Most significantly, outflow structure generated by varying the number of downdrafts, as well as their relative locations and pulsing frequency, were examined. By applying the surge identification algorithm to varying cases and testing its ability to identify prescribed pulsation frequencies, its robustness and utility was determined.

3. RESULTS

The simplest idealized downdraft simulation examined involved a single, pulsing downdraft. The pocket of constant cooling varied in magnitude governed by a sine function with an oscillation period of 400 s. The surge identification technique successfully generated a surge index corresponding with bursts of high outflow velocity relative to the base state (Fig. 3b). The surge flag identified the surges as two-dimensional objects across the domain (Fig. 3c). Resulting statistics (Fig. 4) show a graphical representation of surge production and propagation, with local maxima of surge extent fluctuating at a period of approximately 400 s. This demonstrates the algorithm was able to recover the prescribed pulsing frequency and

agrees with the conceptual model that the frequency of surge generation is directly related to the frequency of downdraft pulsing.

A more complicated situation more closely resembling the complex nature of real supercells included two adjacent downdrafts pulsing at a phase shift of $\frac{\pi}{2}$. This generated alternating downdraft pulses in close enough proximity that outflow air may interact. Each downdraft pulsed at a period of 400 s as in the previous case. Following the same method, the surge index was calculated, and the flagging algorithm identified surges as horizontal momentum perturbations propagating across the analysis subdomain (Fig. 5). Since the subdomain is centered on the location of minimum vertical velocity, the alternating downdrafts create the issue of subdomain shifting. Times where the subdomain center shifts between downdrafts are evident by sharp changes in the integrated horizontal surge coverage (Fig. 6a). However, the frequency of pulsing qualitatively remains similar.

In both cases, and in other simulations not discussed here, a qualitative relationship between maxima in the magnitude of near-ground vertical vorticity and surge generation is visible (Figs. 4a and 4d; Figs. 6a and 6d). The relationship between momentum surges and vertical vorticity extrema has previously been noted by Dahl et al. (2014).

Additional idealized downdraft simulations varied the number, pulse frequency and location of downdrafts and applied the same objective identification algorithm. In each scenario, this technique faithfully identified momentum surges and recovered their frequency of generation.

4. SUMMARY AND DISCUSSION

Work toward a versatile, objective algorithm to identify internal momentum surges has yielded promising early results. By defining surges as storm-relative horizontal velocity perturbations, they may be identified and tracked across a domain, yielding statistics on their frequency of generation, intensity, source

location, and relationship with vertical vorticity. Initial tests with prescribed surge frequencies show promising results. Ongoing work includes implementation of a Fourier decomposition to obtain the surge frequency.

Limitations of this algorithm including appropriate analysis subdomain size and location are being addressed in ongoing work, which includes developing objective definition of the analysis domain size. Finally, it is recognized that different storms may require different thresholds of momentum perturbation to define a surge. This threshold is currently selected manually and usually between 5-15 m s^{-1} , although thunderstorms with very large or very small velocity perturbations may require a different magnitude. Through the study of additional storm simulations, we expect to gain a better understanding of the range of appropriate thresholds in varying storm types.

Future methods of isolating storm regions of interest by analyzing the “flux” of surges around individual downdrafts or near a developing vortex may prove to be more appropriate in obtaining robust surge statistics.

Following testing and fine-tuning of the surge identification algorithm, it will be applied to a wide variety of storm simulations. Different storm environments and microphysics parameterizations will result in a variety of supercells. By identifying and analyzing the surge characteristics of these storms, we hope to gain further insight into surge generation and propagation and investigate the impact of surge-associated vorticity on the generation and maintenance of near-ground vorticity extrema.

5. ACKNOWLEDGEMENTS

The authors would like to acknowledge Dr. George Bryan for the use of CM1 and its source code, Dr. Matthew Parker for supplying code for idealized downdraft simulations, and Dr. Eric Bruning for productive, thought-provoking discussion.

6. REFERENCES

- Brandes, E. A., 1981: Finestructure of the Del City-Edmond Tornadic Mesocirculation. *Mon. Wea. Rev.*, **109**, 635–647.
- Bryan, G. H., J. M. Fritsch, 2002: A benchmark simulation for moist hydrostatic numerical models. *Mon. Wea. Rev.*, **130**, 2917–2928.
- Dahl, J. M. L., M. D. Parker, and L. J. Wicker, 2014: Imported and Storm-Generated Near-Ground Vertical Vorticity in a Simulated Supercell. *J. Atmos. Sci.*, **71**, 3027–3051.
- Davies-Jones, R. P., 1982: Observational and theoretical aspects of tornadogenesis. *Intense Atmospheric Vortices*, L. Bengtsson and J. Lighthill, Eds. Springer-Verlag, 175-189.
- Davies-Jones, R. P., and H. E. Brooks, 1993: Mesocyclogenesis from a theoretical perspective. *The Tornado: Its Structure, Dynamics, Prediction, and Hazards*, Geophys. Monogr., No. 79, Amer. Geophys. Union, 105-114.
- Finley, C. A., and B. D. Lee, cited. 2014: Mobile mesonet observations of an intense RFD and multiple RFD gust fronts in the May 23 Quinter, Kansas tornadic supercell during TWISTEX 2008. [Available online at http://ams.confex.com/ams/24SLS/techprogram/paper_142133.htm].
- Goff, R. C. 1976: Vertical Structure of Thunderstorm Outflows. *Mon. Wea. Rev.*, **104**, 1429–1440.
- Klemp, J. B., and R. Rotunno, 1983: A Study of the Tornadic Region within a Supercell Thunderstorm. *J. Atmos. Sci.*, **40**, 359–377.
- Lee, B. D., C. A. Finley, and T. M. Samaras, 2011: Surface Analysis near and within the Tipton, Kansas, Tornado on 29 May 2008. *Mon. Wea. Rev.*, **139**, 370–386.

Lee, B. D., C. A. Finley, and C. D. Karstens, 2012: The Bowdle, South Dakota, Cyclic Tornadic Supercell of 22 May 2010: Surface Analysis of Rear-Flank Downdraft Evolution and Multiple Internal Surges. *Mon. Wea. Rev.*, **140**, 3419–3441.

Markowski, P. M., 2002: Hook Echoes and Rear-Flank Downdrafts: A Review. *Mon. Wea. Rev.*, **130**, 852–876.

Marquis, J., Y. P. Richardson, J. Wurman, and P. M. Markowski, 2008: Single- and Dual-Doppler Analysis of a Tornadic Vortex and Surrounding Storm-Scale Flow in the Crowell, Texas, Supercell of 30 April 2000. *Mon. Wea. Rev.*, **136**, 5017–5043.

Parker, M. D. and J. M. L. Dahl, 2014: Production of near-surface vertical vorticity by downdrafts. *Mon. Wea. Rev.*, submitted.

Schenkman, A. D., M. Xue, and M. Hu, 2014: Tornadogenesis in a High-Resolution Simulation of the 8 May 2003 Oklahoma City Supercell. *J. Atmos. Sci.*, **71**, 130–154.

Shabbott, C. J., and P. M. Markowski, 2006: Surface In Situ Observations within the Outflow of Forward-Flank Downdrafts of Supercell Thunderstorms. *Mon. Wea. Rev.*, **134**, 1422–1441.

Skinner, P. S., C. C. Weiss, M. M. French, H. B. Bluestein, P. M. Markowski, and Y. P. Richardson, 2014: VORTEX2 Observations of a Low-Level Mesocyclone with Multiple Internal Rear-Flank Downdraft Momentum Surges in the 18 May 2010 Dumas, Texas, Supercell. *Mon. Wea. Rev.*, **142**, 2935–2960.

Trapp, R. J., and M. L. Weisman, 2003: Low-Level Mesovortices within Squall Lines and Bow Echoes. Part II: Their Genesis and Implications. *Mon. Wea. Rev.*, **131**, 2804–2823.

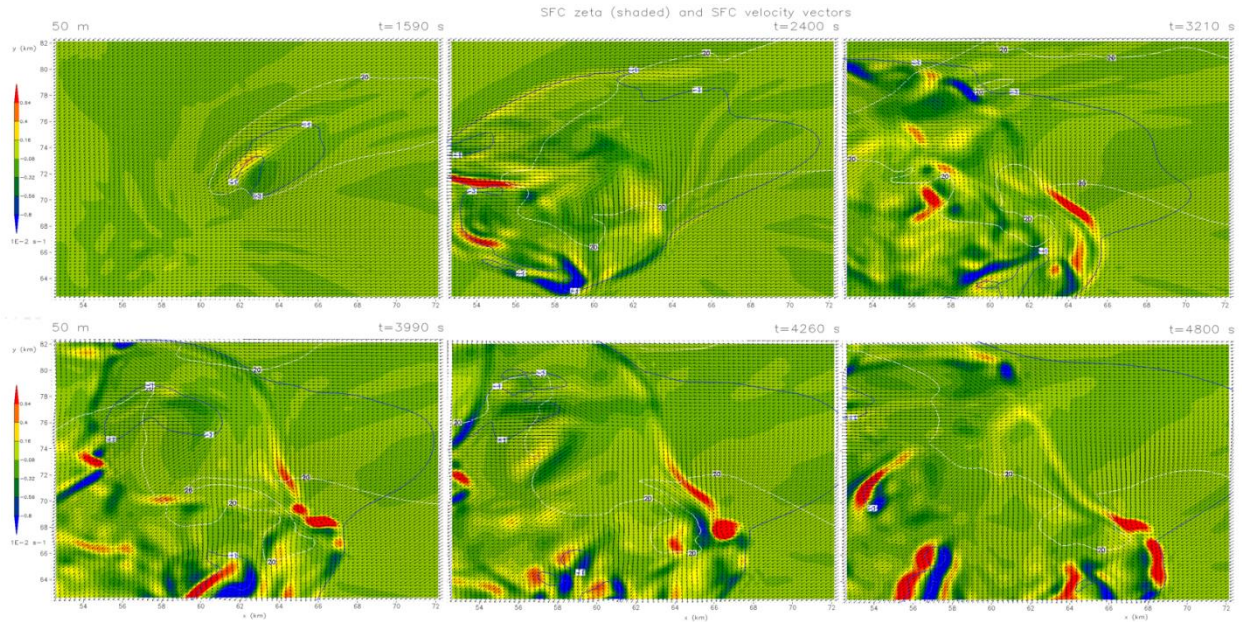


Figure 1. Vertical vorticity (shaded) at 50 m AGL, extent of cold pool defined by -1 K potential temperature perturbation (black contour), and 20 dBZ reflectivity contour (white). Clockwise from top left: $t = 1590$ s, $t = 2400$ s, $t = 3210$ s, $t = 3990$ s, $t = 4260$ s, $t = 4800$ s.

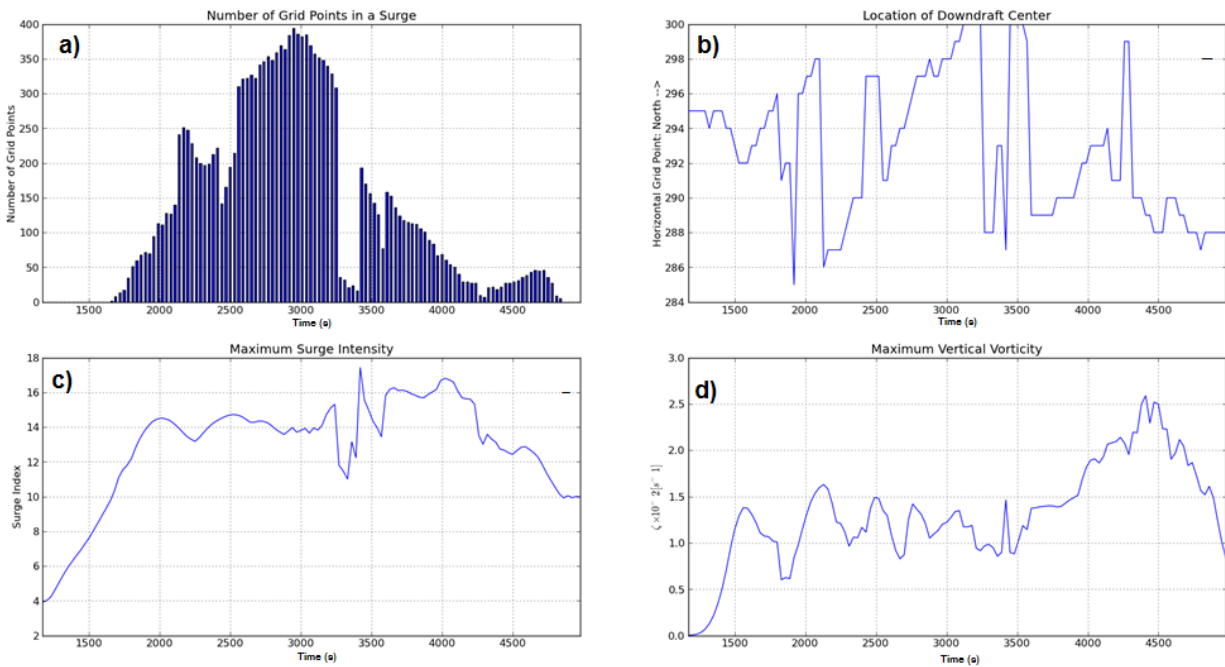


Figure 2. Example output statistics of horizontal momentum surges, as identified by the objective identification algorithm, including (a) total combined horizontal extent of surges in the analysis subdomain, (b) location of primary downdraft source, (c) maximum surge intensity, and (d) maximum vertical vorticity.

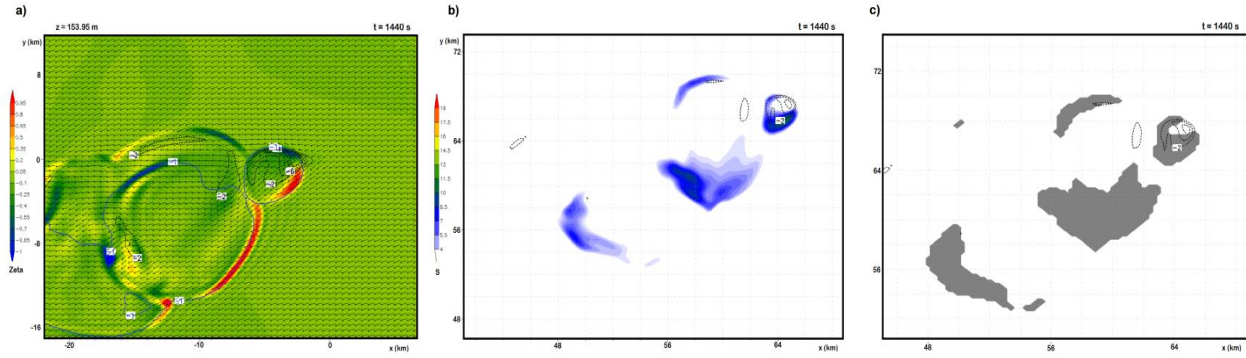


Figure 3. Idealized, isolated, single, pulsing downdraft simulation at lowest model level (50 m AGL) at $t = 1440$ s, with calculated (a) vertical vorticity (shaded), cold pool extent (black contour), and b) surge index (shaded) and downdraft velocity (dashed contour, in m s^{-1}), and (c) binary surge field derived by flagging algorithm with threshold $S = 4 \text{ m s}^{-1}$.

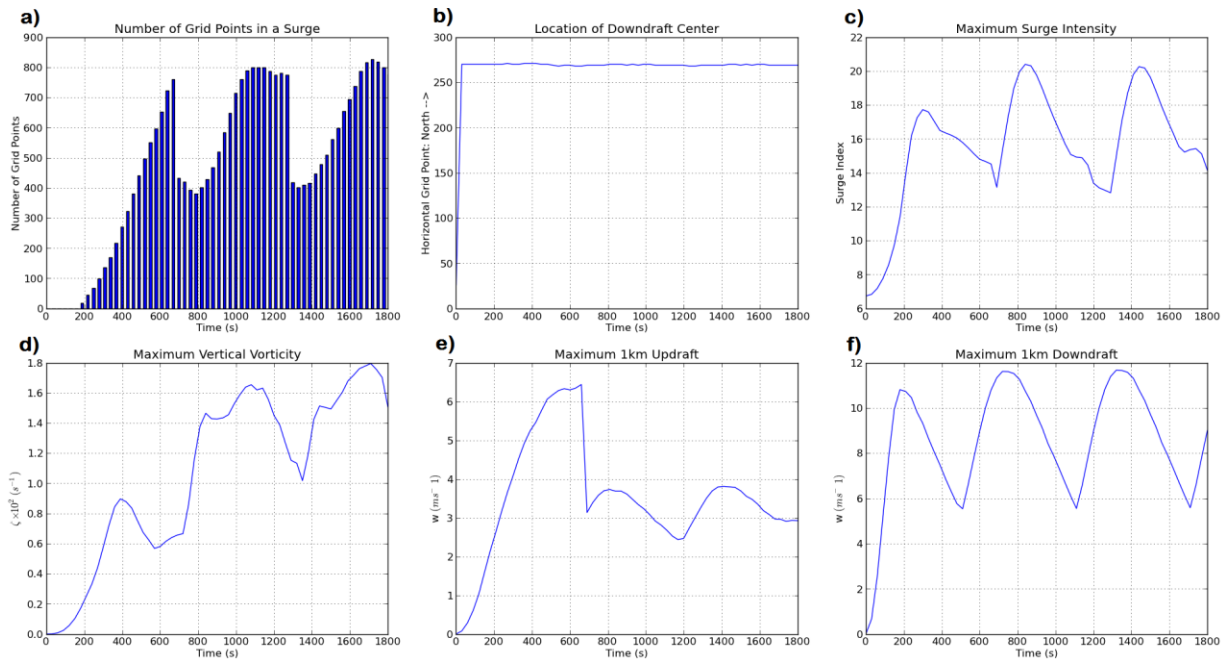


Figure 4. Statistics for the case in Fig. 3, including (a) total combined horizontal extent of surges in the analysis subdomain, (b) location of downdraft source, (c) maximum surge intensity, (d) maximum vertical vorticity, (e) maximum updraft velocity, and (f) maximum downdraft velocity.

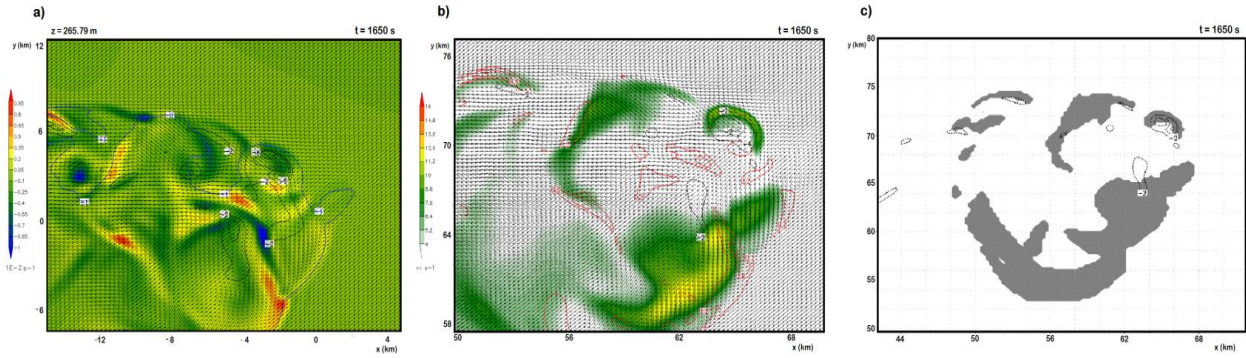


Figure 5. Idealized downdraft simulation at $t = 1650$ s with two adjacent downdrafts pulsing at the same frequency, but with a $\frac{\pi}{2}$ -phase offset. Shown are calculated (a) vertical vorticity (shaded) with cold pool extent (blue contour) and downdraft velocity (black dashed contour), (b) surge index (shaded) with downdraft velocity (dashed contour, in m s^{-1}) and vertical vorticity (red contour, in 10^{-2}s^{-1}), and (c) binary surge field derived by flagging algorithm with threshold $S = 7 \text{ m s}^{-1}$.

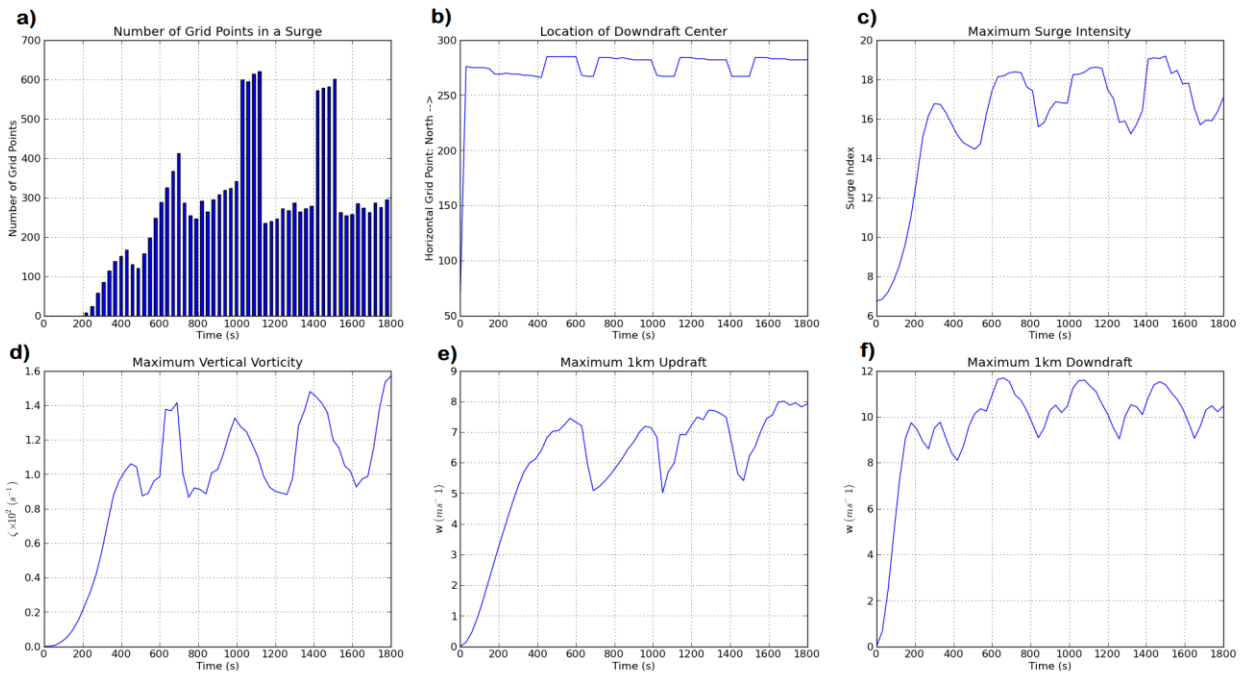


Figure 6. Statistics for the case in Fig. 5, including (a) total combined horizontal extent of surges in the analysis subdomain, (b) location of downdraft source, (c) maximum surge intensity, (d) maximum vertical vorticity, (e) maximum updraft velocity, and (f) maximum downdraft velocity.